

Etherification of *tert*-Amyl Alcohol with Methanol over Ion-Exchange Resin

G. D. Yadav* and A. V. Joshi

Chemical Engineering Division, University Department of Chemical Technology (UDCT), Matunga, Mumbai - 400 019, India

Abstract:

tert-Amyl methyl ether (TAME) is a proven high octane additive. The synthesis of *tert*-amyl methyl ether from *tert*-amyl alcohol and methanol has been carried out in the presence of a variety of solid acid catalysts. Amberlyst-36 was found to be very effective in comparison with other solid acids. A complete theoretical and experimental analysis is presented for the model studies of *tert*-amyl alcohol with methanol. The parallel reactions of *tert*-amyl alcohol adsorbed on the sites were found to control the overall rate of reaction, which led to the formation of TAME, 2-methyl-1-butene (2MB1), and 2-methyl-2-butene (2MB2). The reaction follows pseudo-first-order kinetics at a fixed catalyst loading. The individual rate constants for the formation of TAME, 2MB1, and 2MB2 were also evaluated from the same data.

Introduction

Synthesis of alkyl-*tert*-alkyl ethers by reactions of isoolefins with alcohols is an efficient process, and these ethers are increasingly being used as ecologically clean additives to motor oils. *tert*-Alkyl ethers, namely, methyl-*tert*-butyl ether (MTBE) and ethyl-*tert*-butyl ether (ETBE) are produced on industrial scale as nontoxic and high-octane gasoline additives. Production of *tert*-amyl methyl ether (TAME) has been investigated in recent years.¹ *tert*-Amyl methyl ether (TAME) with an octane number of 106 which is almost the same as that of MTBE (109) can be employed as a possible high-octane additive to motor fuels. The blending Reid vapour pressure (RVP) of TAME is 1 psi, which is much lower than that of MTBE (8 psi) and ETBE (4 psi). Thus, TAME shows a lot of promise as a fuel additive particularly since MTBE is under close scrutiny and California has already banned the usage of MTBE as an octane booster.

Synthesis of *tert*-alkyl ethers by etherification process using cation-exchange resins,^{2–6} acid catalysts,^{7,8} zeolites,⁹

and sheet silicate.¹⁰ Linnekoski et al.¹¹ have reported simultaneous isomerization and etherification of isoamylenes with alkanols. Safronov et al.¹² have studied thermodynamics of the synthesis of TAME. Rihko and Krause¹³ determined the reaction rates in liquid phase in a continuous stirred tank reactor. Oost and Hoffmann¹⁴ studied the influence of internal and external mass-transfer resistance in the synthesis of TAME in a continuous-flow recycle reactor. Goto et al.^{15–17} synthesized MTBE and ETBE at atmospheric conditions by a condensation reaction of methanol or ethanol with *tert*-butyl alcohol. To achieve continuous production of MTBE and ETBE, Goto et al.^{18,19} employed reactive distillation combined with pervaporation.

Etherification of *tert*-amyl alcohol to produce TAME was thus considered as an important problem necessitating the use of different solid acid catalysts. Synthesis of MTBE from *tert*-butyl alcohol and methanol has been studied in this laboratory by using a variety of solid acids. Heteropoly acids (HPA) supported on clays have shown superior activity as catalysts in comparison to others in the alkylation and etherification reactions.²⁰

Experimental Section

Chemicals. K-10 clay was obtained from Aldrich, U.S.A., and Filtrol-24 from Fluka, Germany. Zirconium oxychloride, dodecatungstophosphoric acid, 1,4-dioxane, and methanol were obtained from M/s s.d. Fine Chemicals Pvt. Ltd., Mumbai, India. *tert*-Amyl alcohol was obtained from Acros, U.S.A. Amberlyst-15 and Amberlyst-36 were procured from Rohm and Haas, U.S.A. All chemicals were of analytical grade and used without further purification.

Catalysts. Dodecatungstophosphoric acid (DTP) supported on K-10 was prepared by a well-established procedure in our laboratory.²¹ A desired quantity of montmorillonite clay (K10) was taken and dried in an oven for 2 h, and dodecatungstophosphoric acid dissolved in methanol was added dropwise, with stirring to prepare the catalyst by the

* To whom correspondence should be addressed.

- (1) Ignatius, J.; Jarvelin, H.; Lindqvist, P. *Hydrocarbon Process* **1995**, 74(2), 51.
- (2) Adams, J. R.; Smith, L. A., Jr.; Hearn, D.; Jones, E. M., Jr.; Arganbright, R. P. U.S. Patent 5,792,891, 1998; *Chem. Abstr.* **1998**, 129, 150345.
- (3) Jarvelin, H.; Lindqvist P.; Tamminen, E. U.S. Patent 5,852,220, 1998; *Chem. Abstr.* **1999**, 130, 53953.
- (4) Yang, B. L.; Maeda, M.; Goto, S. *Int. J. Chem. Kinet.* **1998**, 30(2), 137.
- (5) Chodorge, J. A.; Commereuc, D.; Cosyns, J.; Duee D.; Jorck, B. Eur. Patent 742,195, 1996; *Chem. Abstr.* **1997**, 126, 46874.
- (6) Piccoli, R. L.; Lovisi, H. R. *Ind. Eng. Chem. Res.* **1995**, 34, 510.
- (7) Marion, M. C.; Viltard, J. C.; Travers, P.; Harter, I.; Forestiere, A. Eur. Patent 755,706, 1997; *Chem. Abstr.* **1997**, 126, 200887.
- (8) Hoffmann, U.; Krummradt, H.; Rapmund, P.; Sundmacher, K. *Chem. Ing. Technol.* **1997**, 69(4), 483; *Chem. Abstr.* **1997**, 127, 6854.
- (9) Miller, S. J. U.S. Patent 5,801,293, 1998; *Chem. Abstr.* **1998**, 129, 177197.

- (10) Fleitas, D. H.; Macanio, H. R.; Perez, C. F.; Orio, O. A. *React. Kinet. Catal. Lett.* **1991**, 43, 183.
- (11) Linnekoski, J. A.; Kiviranta, P. P.; Krause, A. O.; Rihko-Struckmann, L. K. *Ind. Eng. Chem. Res.* **1999**, 38(12), 4563.
- (12) Safronov, V. V.; Sharonov, K. G.; Rozhnov, A. M.; Alenin, V. I.; Sidorov, S. A. *J. Appl. Chem. USSR* **1989**, Part 1, 62(4), 763.
- (13) Rihko, L. K.; Krause, A. Outi I. *Ind. Chem. Eng. Res.* **1995**, 34, 1172.
- (14) Oost, C.; Hoffmann, U. *Chem. Eng. Technol.* **1995**, 18, 203.
- (15) Matouq, M. H.; Goto, S. *Int. J. Chem. Kinet.* **1993**, 25, 825.
- (16) Matouq, M. H.; Tagawa, T.; Goto, S. *J. Chem. Eng. Jpn.* **1993**, 26, 254.
- (17) Yin, X. D.; Yang, B. L.; Goto, S. *Int. J. Chem. Kinet.* **1995**, 27, 1065.
- (18) Matouq, M.; Tagawa, T.; Goto, S. *J. Chem. Eng. Jpn.* **1993**, 27, 302.
- (19) Yang, B. L.; Goto, S. *Sci. Sep. Technol.* **1995**, 32(5), 971.
- (20) Yadav, G. D.; Kirthivasan, N. *J. Chem. Soc., Chem. Commun.* **1995**, 203.
- (21) Yadav, G. D.; Kirthivasan, N. *Appl. Catal., A* **1997**, 154, 29.

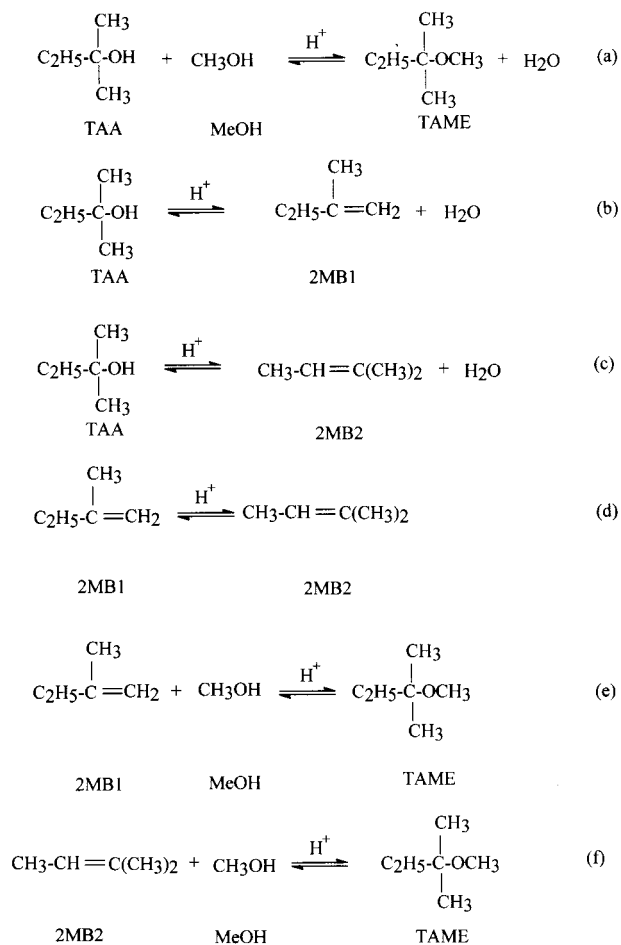


Figure 1. Reaction scheme for etherification of *tert*-amyl alcohol with methanol.

so-called incipient wetness technique. Sulphated zirconia was also prepared by an established procedure.²²

Reaction Procedure. All experiments were carried out in a 100 mL stainless steel autoclave manufactured by Parr Instruments Co., U.S.A. A four-bladed-pitched turbine impeller was used for agitation. The temperature was maintained at ± 1 °C of the desired value with the help of an in-built proportional-integral-derivative (PID) controller. Predetermined quantities of reactants and the catalyst were charged into the autoclave, and the temperature was raised to the desired value.

In a typical experiment, 0.1 mol of *tert*-amyl alcohol and 0.5 mol of methanol were used, and 1,4-dioxane was added to make the total volume to 50 cm³. A standard catalyst loading of 1.0 g was used at 70 °C. The reaction mixture was allowed to reach the desired temperature, and the initial/zero time sample was collected. Agitation was commenced and maintained at a particular speed. Samples were withdrawn periodically for analysis.

Analysis. Analysis of the reaction mixture was done on a G. C. (Chemito 8510) with 10% SE-30 column (4 m \times 3.18 mm) and FID.

Samples were analysed for methanol, *tert*-amyl alcohol, and 2-methyl-1-butene, 2-methyl-2-butene, and *tert*-amyl

Table 1. Efficacies of various catalysts on conversion of *tert*-amyl alcohol^a

catalyst	% conversion	% yield ^b of TAME	selectivity ^c
Amberlyst-15	82	44.0	0.644
Amberlyst-36	86.8	44.7	0.701
DTP	74.3	9.4	0.0762
Filtrol-24	37	25.0	0.123
K-10	51.2	6.1	0.0325
20% DTP/K-10	58.3	5.6	0.0346

^a *tert*-Amyl alcohol:methanol: 1:2; catalyst loading: 0.02 g/cm³; time: 4 h; temperature: 70 °C; speed of agitation: 800 rpm; solvent: 1,4-dioxane. ^b Yield = amount of TAME formed/amount of *tert*-amyl alcohol reacted. ^c Selectivity = rate of TAME formation/rate of formation of 2MB1 and 2MB2.

methyl ether. Identification of products was done by GC-MS.

Reaction Scheme. There are six possible reactions that can take place in the presence of acid catalyst as shown in Figure 1. However, the dimers of 2-methyl-1-butene (2MB1) and 2-methyl-2-butene (2MB2) were not detected. This observation was helpful in devising a reaction mechanism.

Results and Discussion

Efficacies of Various Catalysts. Various solid acid catalysts were employed to evaluate their effectiveness in this reaction. A 0.02 g/cm³ loading of catalyst based on the organic volume of the reaction mixture was taken at 70 °C. The mole ratio of *tert*-amyl alcohol to methanol was kept at 1:2, with an agitation speed of 800 rpm. The catalysts used were K-10 montmorillonite, dodecatungstophosphoric acid, 20% DTP/K-10, sulphated zirconia, Filtrol-24, Amberlyst-15, and Amberlyst-36. Table 1 shows conversion of *tert*-amyl alcohol, the limiting reactant, for the various catalysts. Amberlyst-36 was the most active for the conversion of *tert*-amyl alcohol compared to other catalysts and had better selectivity towards *tert*-amyl methyl ether. Amberlyst-15 gave lesser conversion than Amberlyst-36 with almost the same selectivity towards TAME. Amberlyst-36 has an ion-exchange capacity of 5.45 mequiv, which is greater than that of Amberlyst-15 of 4.9 mequiv. Being a soluble catalyst, DTP gave good conversion but poor selectivity for TAME. It should be recognized that the homogeneous catalyst DTP was almost 5 times of 20% DTP/K10 and also not reusable at the same catalyst loading. K-10 and 20% DTP/K-10 gave less conversion than Amberlyst-36, which may be because they have lesser ion-exchange capacity. S-ZrO₂ is a Lewis acid and hence is less effective. One of the reasons for the high conversion of *tert*-amyl alcohol is the formation of the gaseous 2MB1 and 2MB2, which have boiling points of 304 and 311 K, respectively, and do not reach equilibrium. In all further experiments Amberlyst-36 was used as the catalyst.

Effect of Speed of Agitation. To evaluate the role of external mass transfer on the reaction rate, the effect of the speed of agitation was studied. The speed of agitation was varied from 800 to 1200 rpm (Figure 2). It was observed that the conversion of *tert*-amyl alcohol was practically the same in all of the cases without any change in selectivity. Thus, it was ascertained that the external mass-transfer effects

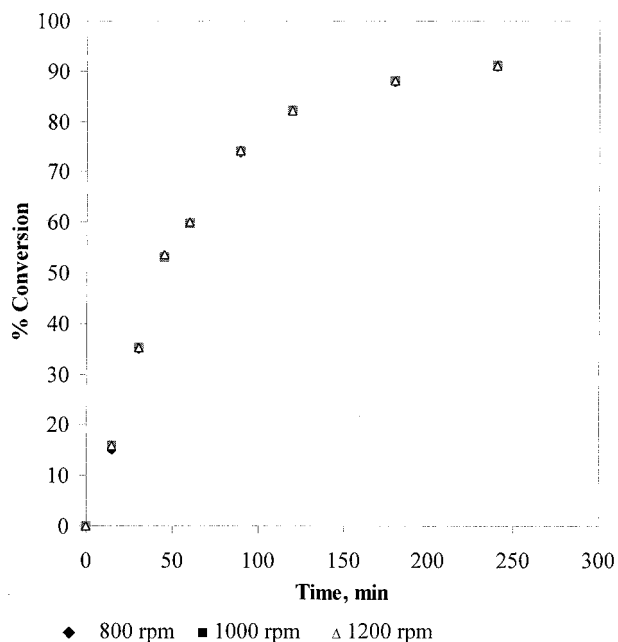
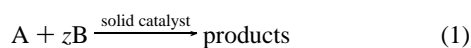


Figure 2. Effect of speed of agitation on conversion of *tert*-amyl alcohol.

did not influence the rate of reaction. All further reactions were carried out at 800 rpm. A theoretical analysis of the assessment of external mass-transfer resistance is given to support this observation. Details of this theory for general slurry reactions are given elsewhere.²²

This is a typical solid–liquid slurry reaction involving the transfer of *tert*-amyl alcohol, the limiting reactant (A), and methanol (B) from the bulk liquid phase to the catalyst wherein external mass transfer of reactants to the surface of the catalyst particle takes place, followed by intraparticle diffusion, adsorption, surface reactions, and desorption. The resistance due to external solid–liquid mass transfer and intraparticle diffusion limitation should be eliminated before a true kinetic model can be developed.



At steady state, the rate of mass transfer per unit volume of the liquid phase ($\text{gmol} \cdot \text{cm}^{-3} \cdot \text{s}^{-1}$) is given by:

$$R_A = k_{\text{SL-A}} a_p \{ [A_o] - [A_s] \} \quad (2)$$

(rate of transfer of A from bulk liquid to external surface
of the catalyst particle)

$$= z k_{\text{SL-B}} a_p \{ [B_o] - [B_s] \} \quad (3)$$

(rate of transfer of B from the bulk liquid phase to the
external surface of the catalyst particle) ($z = 1$ in this case)

$$= r_{\text{obs}} \text{ (observed rate of reaction within the catalyst particle)} \quad (4)$$

Here the subscripts “o” and “s” denote the concentrations in bulk liquid phase and external surface of catalyst, respectively.

Depending on the relative magnitudes of external resistance to mass transfer and reaction rates, different controlling

mechanisms have been put forward.²³ When the external mass-transfer resistance is small, then the following inequality holds,

$$1/r_{\text{obs}} \gg 1/k_{\text{SL-A}} a_p [A_o] \text{ and } 1/k_{\text{SL-B}} a_p [B_o] \quad (5)$$

The observed rate r_{obs} could be given by three types of models wherein the contribution of intraparticle diffusional resistance could be accounted for by incorporating the effectiveness factor η . These models are:

- The Power Law model if there is very weak adsorption of reactant species,
- Langmuir–Hinselwood–Hougen–Watson model,
- Eley–Rideal model.

It was therefore necessary to study the effects of speed of agitation and catalyst loading to ascertain the absence of external and intraparticle resistance so that a true intrinsic kinetic equation could be used. Since the conversion was found to remain practically the same in the range of 800–1200 rpm, it indicated the absence of external solid–liquid mass-transfer resistance. Theoretical analysis was also done to ensure that the external mass-transfer resistance was indeed absent as delineated below.

According to eq 5, it is necessary to calculate the rates of external mass transfer of *tert*-amyl alcohol (A) and methanol (B) and compare them with the rate of reaction.

For a typical spherical particle, the particle surface area per unit liquid volume is given by

$$a_p = 6w/(\rho_p d_p) \quad (6)$$

where w = catalyst loading g/cm^3 of liquid phase, ρ_p = density of particle g/cm^3 , and d_p = particle diameter, cm.

For *tert*-amyl alcohol etherification, at a catalyst loading of $0.02 \text{ g}/\text{cm}^3$ and the particle size (d_p) of 0.03 cm, the calculated value of $a_p = 4.21 \text{ cm}^2/\text{cm}^3$ of the liquid phase. The liquid-phase diffusivity values of the reactants A (*tert*-amyl alcohol) and B (methanol), denoted by D_{AB} and D_{BA} , were calculated using the Wilke–Chang equation²⁴ at 70°C as 3.494×10^{-5} and $2.204 \times 10^{-5} \text{ cm}^2/\text{s}$, respectively. The solid–liquid mass transfer coefficients for both A and B were calculated from the limiting value of the Sherwood number (e.g. $Sh_A = k_{\text{SL-A}} d_p / D_{\text{AB}}$) of 2. The actual Sherwood numbers are typically higher by order of magnitude in well-agitated systems but for conservative estimations a value of 2 is taken.^{22–23} The solid–liquid mass-transfer coefficients $k_{\text{SL-A}}$ and $k_{\text{SL-B}}$ values were obtained as 2.329×10^{-3} and $1.469 \times 10^{-3} \text{ cm}/\text{s}$, respectively. The initial rate of reaction was calculated from the conversion profiles. A typical calculation shows that for a standard reaction the initial rate was calculated as $3.33 \times 10^{-7} \text{ gmol}/\text{cm}^3 \cdot \text{s}$. Therefore, putting the appropriate values in eq 5:

$$1/r_{\text{obs}} \gg 1/k_{\text{SL-A}} a_p [B_o] \text{ and } 1/k_{\text{SL-B}} a_p [B_o]$$

$$\text{i.e., } 3 \times 10^6 \gg 5.098 \times 10^4 \text{ and } 1.617 \times 10^4 \quad (7)$$

(23) Kumbhar, P. S.; Yadav, G. D. *Chem. Eng. Sci.* **1989**, *44*, 2535.

(24) Reid, R. C.; Prausnitz, M. J.; Sherwood, T. K. *The Properties of Gases and Liquids*, 3rd ed.; McGraw-Hill Book Company: New York, 1977.

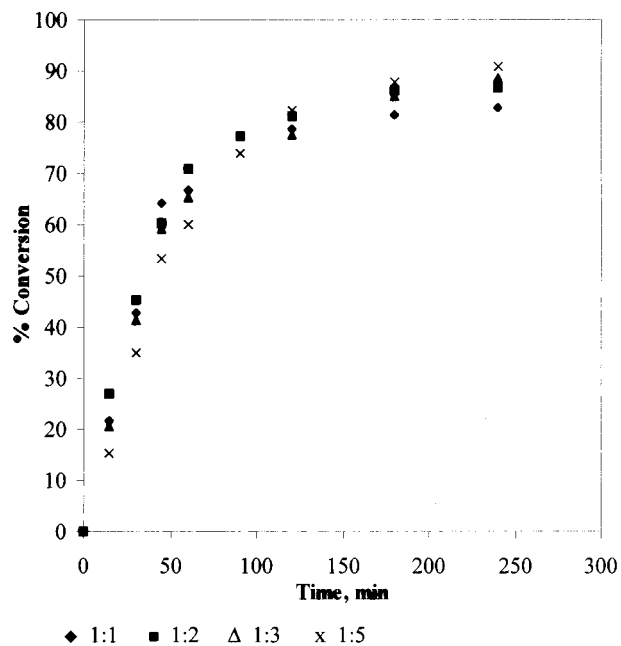


Figure 3. Effect of mole ratio on conversion of *tert*-amyl alcohol.

Table 2. Effect of mole ratio on conversion of *tert*-amyl alcohol^a

<i>tert</i> -amyl alcohol:methanol	% conversion	% yield of TAME	selectivity
1:1	82.9	36.17	0.469
1:2	86.8	44.7	0.701
1:3	88.7	60.8	1.375
1:5	90.7	68.2	1.945

^a Catalyst: Amberlyst-36; temperature: 70 °C; speed of agitation: 800 rpm; time: 4 h; catalyst loading: 0.02 g/cm³; solvent: 1,4-dioxane.

The above inequality demonstrates that there is an absence of resistance due to the solid–liquid external mass transfer for both the species A and B and the rate may be either surface reaction-controlled or intraparticle diffusion-controlled. Therefore, the effects of catalyst loading at a fixed particle size and temperature were studied to evaluate the influence of intraparticle resistance.

Effect of Mole Ratio. The effect of the variation of the mole ratio of *tert*-amyl alcohol to methanol was studied from 1:1 to 1:5 mol under otherwise similar conditions. The conversion of *tert*-amyl alcohol increased from 82.9 to 90.7% as the mole ratio of *tert*-amyl alcohol to methanol was increased from 1:1 to 1:5 (Figure 3). With an increase in the mole ratio of *tert*-amyl alcohol to methanol from 1:1 to 1:5, the dehydration rate of *tert*-amyl alcohol decreases, and hence a significant increase in selectivity towards *tert*-amyl methyl ether from 36.2 to 68.2% was observed⁴ (Table 2). All further experiments were carried out at *tert*-amyl alcohol-to-methanol mole ratio of 1:5.

Effect of Catalyst Loading. In the absence of external mass-transfer resistance, the rate of reaction is directly proportional to catalyst loading based on the entire liquid-phase volume. The loading of catalyst was varied over a range of 0.005–0.02 g/cm³ on the basis of total volume of

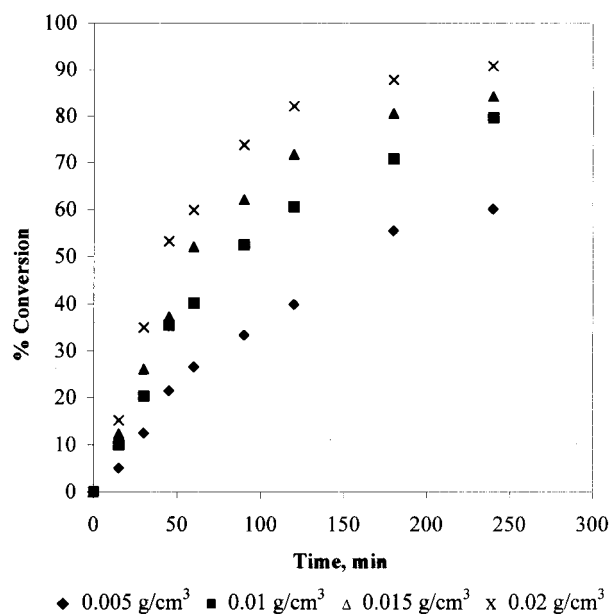


Figure 4. Effect of catalyst loading on conversion of *tert*-amyl alcohol.

Table 3. Effect of catalyst loading on conversion of *tert*-amyl alcohol

catalyst loading (g/cm ³)	% conversion	% yield of TAME
0.005	60.2	66.41
0.01	79.6	67.05
0.015	84.2	67.79
0.02	90.71	68.2

^a *tert*-Amyl alcohol:methanol: 1:5; temperature: 70 °C; solvent: 1,4-dioxane; speed of agitation: 800 rpm; time: 4 h; catalyst: Amberlyst-36.

the reaction mixture. Figure 4 shows the effect of catalyst loading on the conversion of *tert*-amyl alcohol. The conversion increases appreciably with an increase in catalyst loading from 0.005 to 0.01 g/cm³, which is obviously due to the proportional increase in the number of active sites. With further increase in the catalyst loading from 0.01 to 0.02 g/cm³, the conversion increases marginally (Table 3). All further experiments were carried out at 0.02 g/cm³ of catalyst loading.

As shown by eqs 1 and 2, at steady state, the rate of external mass transfer (i.e., from the bulk liquid phase in which A and B are located with concentration [A_o] and [B_o], respectively) to the exterior surface of the catalyst is proportional to *a_p*, the exterior surface area of the catalyst where the concentrations of A and B are [A_s] and [B_s], respectively. For a spherical particle, *a_p* is also proportional to *w*, the catalyst loading per unit liquid volume as shown by eq 6. It is possible to calculate the values of [A_s] and [B_s]. For instance,

$$k_{SL-A}a_p\{[A_o] - [A_s]\} = r_{obs} \quad \text{at steady state}$$

$$= 3.33 \times 10^{-7} \text{ gmol} \cdot \text{cm}^{-3} \cdot \text{s}^{-1} \quad (8)$$

Thus, putting the appropriate values, it is seen that [A_s] ≈ [A_o]. Similarly [B_s] ≈ [B_o]. Thus, any further addition of

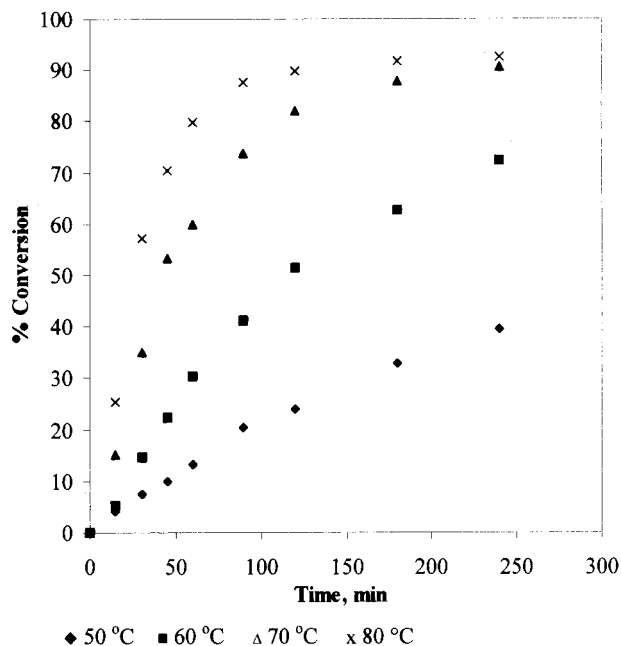


Figure 5. Effect of temperature on conversion of *tert*-amyl alcohol.

catalyst is not going to be of any consequence for changing the rate of external mass transfer.

Proof of Absence of Intraparticle Resistance. The average particle diameter of the catalyst used in the reactions was 0.03 cm, and thus a theoretical calculation was done based on the Wiesz–Prater criterion to assess the influence of intraparticle diffusional resistance.²⁵

According to the Wiesz–Prater criterion, the dimensionless parameter C_{wp} , which represents the ratio of the intrinsic reaction rate to intraparticle diffusion rate, can be evaluated from the observed rate of reaction, the particle radius (R_p), effective diffusivity of the limiting reactant (D_e), and concentration of the reactant at the external surface of the particle.

$$(i) \text{ If } C_{wp} = r_{obs} \rho_p R_p^2 / D_e [A_s] \gg 1$$

then the reaction is limited by severe internal diffusional resistance.

$$(ii) \text{ If } C_{wp} \ll 1,$$

then the reaction is intrinsically kinetically controlled.

The effective diffusivity of *tert*-amyl alcohol (D_{e-A}) inside the pores of the catalyst was obtained from the bulk diffusivity (D_{AB}), porosity (ϵ), and tortuosity (τ), where $D_{e-A} = D_{AB} \cdot \epsilon / \tau$. In the present case, the value of C_{wp} was calculated as 0.0079 for the initial observed rate, and therefore the reaction is intrinsically kinetically controlled. A further proof of the absence of the intraparticle diffusion resistance was obtained through the study of the effect of temperature, and it will be discussed later.

Effect of Temperature. The effect of temperature on conversion under otherwise similar conditions was studied

Table 4. Effect of temperature on conversion of *tert*-amyl alcohol^a

temperature (°C)	% conversion	% yield of TAME
50	39.5	61.36
60	72.3	67.7
70	90.7	68.2
80	92.5	71.37

^a Catalyst: Amberlyst-36; *tert*-amyl alcohol:methanol: 1:5; solvent: 1,4-dioxane; time: 4 h; speed of agitation: 800 rpm; catalyst loading: 0.02 g/cm³.

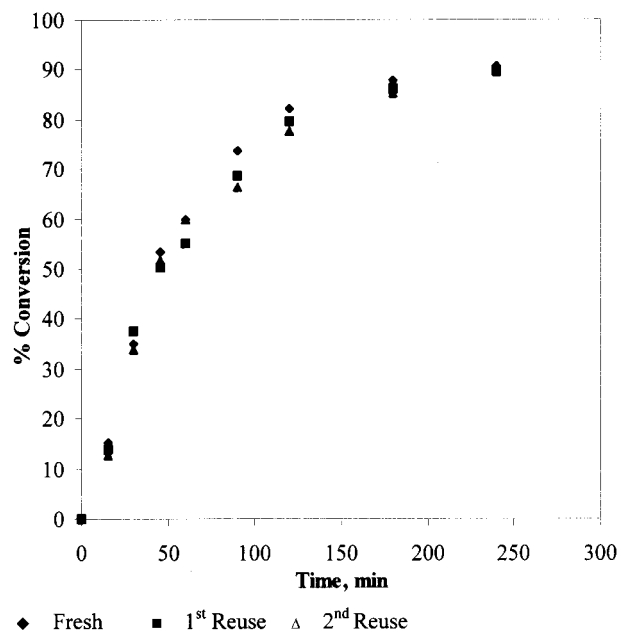


Figure 6. Effect of reusability of catalyst.

in the temperature range of 50–80 °C (Figure 5). The conversion was found to increase substantially with an increase in temperature from 50 to 70 °C. With further increase in temperature from 70 to 80 °C, the conversion increases only slightly as shown in (Table 4). The selectivity to TAME also increases with temperature although marginally. This is likely to be due to different activation energies for the three parallel reactions of TAA. It appears that reaction (a) has higher activation energy (Figure 1). All further experiments were carried out at 70 °C.

Reusability of Amberlyst-36. The reusability of Amberlyst-36 was verified by employing it three times. After each run the catalyst was washed thoroughly with methanol, dried in an oven at 120 °C for 2 h, and weighed. The results are shown in Figure 6. In the presence of fresh catalyst, the conversion of *tert*-amyl alcohol was 90.7%. During the third run, the conversion of *tert*-amyl alcohol was 89.5%, which is almost the same as in the first run, without any significant change in the selectivity of TAME (Table 5). Thus, the catalyst was reusable.

Mechanism and Reaction Kinetics. Analysis of the effect of various parameters and the product profile suggests that the chemisorption of TAA should be the first step followed by other reactions.

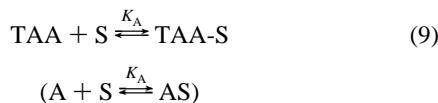
(25) Fogler, H. S. *Elements of Chemical Reaction Engineering*; Prentice-Hall: New Delhi, 1995.

Table 5. Effect of Reusability of Amberlyst-36^a

run number	% conversion	% yield of TAME
1	90.7	68.2
2	90	72.5
3	89.5	71.6

^a *tert*-Amyl alcohol:methanol:1:5; temperature: 70 °C; solvent: 1,4-dioxane; speed of agitation: 800 rpm; time: 4 h; catalyst loading: 0.02 g/cm³.

Chemisorption of TAA:

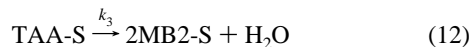
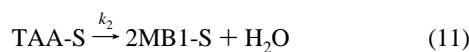


where S is the vacant site

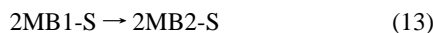
The chemisorbed species reacts according to the following three paths



In the above reaction, the Eley–Rideal mechanism is assumed to be operative since no dimethyl ether was formed.



The following isomerisation reaction is also likely to occur



All of the surface species desorb into the liquid phase in the pore space followed by diffusion out of the particle.

The adsorption equilibrium constants for various species can be written accordingly.

If the parallel forward reactions 10, 11, and 13 of TAA are assumed to control the overall rate of the reaction, then:

$$-r_A = \frac{-dC_A}{dt} = k_1 C_{\text{TAA-S}} C_{\text{MeOH}} + k_2 C_{\text{TAA-S}} + k_3 C_{\text{TAA-S}} \quad (14)$$

$$= (k_1 C_B + k_2 + k_3) C_{\text{AS}} \quad (15)$$

The concentration C_S of the vacant sites

$$\begin{aligned} C_t &= C_S + C_{\text{AS}} + C_{\text{BS}} + C_{2\text{MB1-S}} + C_{2\text{MB2-S}} \\ &= C_S [1 + K_A C_A + K_B C_B + K_{2\text{MB1}} C_{2\text{MB1}} + K_{2\text{MB2}} C_{2\text{MB2}}] \end{aligned} \quad (16)$$

$$\therefore C_S = \frac{C_t}{1 + \sum K_i C_i} \quad (17)$$

C_S can be written in terms of the concentration of catalyst, typically expressed as w in g/cm³, without loss of generality:

$$\therefore C_S = \frac{w}{1 + \sum K_i C_i} \quad (18)$$

$$r_A = \frac{-dC_A}{dt} = \frac{(k_1 C_B + k_2 + k_3) K_A C_A w}{1 + \sum K_i C_i} \quad (19)$$

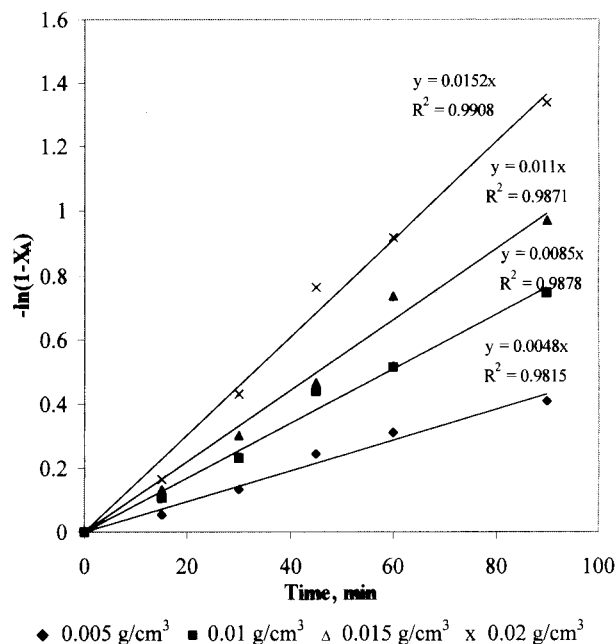


Figure 7. Plot of $-\ln(1 - X_A)$ vs time at different catalyst loadings.

However, $C_{B_0} \gg C_{A_0}$, the initial concentration, and if $\sum K_i C_i \ll 1$, then the above equation becomes

$$\frac{-dC_A}{dt} = k'_1 C_A w$$

where k'_1 = pseudo-first-order rate constant based on the catalyst loading

$$= (k_1 C_{B_0} + k_2 + k_3) K_A \quad (20)$$

k'_1 has units of (cm³/g·mol·sec)(cm³/g-cat).

The above equation can be integrated to get a typical first order form

$$-\ln(1 - X_A) = k'_1 w t = k''_1 \quad (21)$$

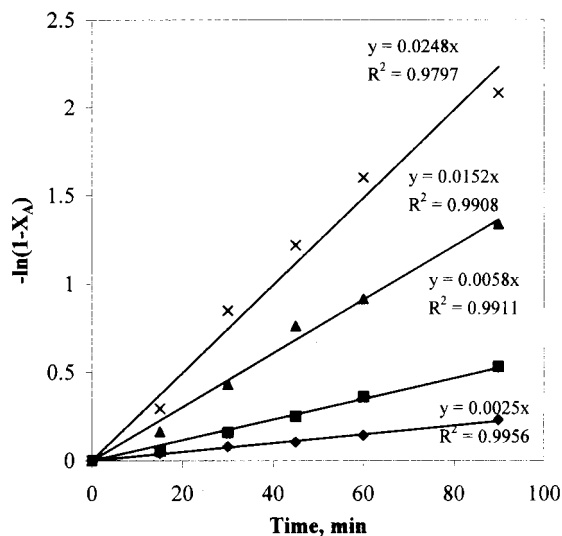
Thus plots can be made of LHS against t for a fixed catalyst value of w to get the rate of constant k''_1 . Once again plots of k''_1 versus w will give k'_1 . The Arrhenius plot of k'_1 versus $1/T$ can be made under otherwise similar conditions to get activation energy, which will be an apparent value.

Equation 20 can also be written as follows:

$$\begin{aligned} k'_1 &= k_1 K_A C_{B_0} + k_2 K_A + k_3 K_A \\ &= k_{c1} C_{B_0} + k_{c2} + k_{c3}, \quad \text{respectively} \end{aligned} \quad (22)$$

In fact, the individual combined rate constants k_{c1} , k_{c2} , and k_{c3} , which include K_A , could be calculated from the rates of formations of TAME, 2MB1, and 2MB2 since the product distribution was known. These values were calculated as $k_{c1} = 0.508 \text{ cm}^{-6} \cdot \text{gmol}^{-1} \cdot \text{s}^{-1} \cdot \text{g-cat}^{-1}$; and $k_{c2} = 3.92 \times 10^{-4}$ and $k_{c3} = 2.84 \times 10^{-3} \text{ cm}^{-3} \cdot \text{s}^{-1} \cdot \text{g-cat}^{-1}$

In the above theory, it is assumed that methanol is not strongly adsorbed to generate the dehydrated product dimethyl ether.



◆ 50 °C ■ 60 °C ▲ 70 °C × 80 °C

Figure 8. Plot of $-\ln(1 - X_A)$ vs time at different temperatures.

Plots of $-\ln(1 - X_A)$ versus time for *tert*-amyl alcohol were made for different catalyst loading as shown in Figure 7. The equation fits the data quite well because the R^2 values are very high, >0.98 . Similar plots were made at different temperatures, and it was found that the data fit well and the reaction conforms to the proposed model (Figure 8). The Arrhenius plots of $\ln k_1'$ versus T^{-1} were made to get the apparent energy of activation as 17.94 kcal/mol (Figure 9), thereby also suggesting the reaction was intrinsically kinetically controlled. The reaction follows a pseudo first-order kinetics at fixed catalyst loading.

Selectivity of TAME. The point selectivity values for the formation of TAME vis-à-vis 2MB1 and 2MB2 are given by

$$S_{\text{TAME}/(2\text{MB1}+2\text{MB2})} = \frac{\frac{dC_{\text{TAME}}}{dt}}{\frac{dC_{2\text{MB1}}}{dt} + \frac{dC_{2\text{MB2}}}{dt}} = \frac{k_1 C_{\text{MeOH}} C_{\text{TAA-S}}}{k_2 C_{\text{TAA-S}} + k_3 C_{\text{TAA-S}}} \quad (23)$$

$$S_{\text{TAME}/(2\text{MB1}+2\text{MB2})} = \frac{dC_{\text{TAME}}}{dC_{2\text{MB1}} + dC_{2\text{MB2}}} = \left(\frac{k_1}{k_2 + k_3} \right) C_{\text{MeOH}} \quad (24)$$

$$S_{\text{TAME}/(2\text{MB1}+2\text{MB2})} = \frac{\Delta C_{\text{TAME}}}{\Delta C_{2\text{MB1}} + \Delta C_{2\text{MB2}}} = \frac{C_{\text{TAME}-0} - C_{\text{TAME}}}{C_{2\text{MB1}} + C_{2\text{MB2}}} = \frac{X_A C_{\text{TAME}-0}}{C_{2\text{MB1}} + C_{2\text{MB2}}} \quad (25)$$

$$S_{\text{TAME}/(2\text{MB1}+2\text{MB2})} = \left(\frac{k_1}{k_2 + k_3} \right) C_{\text{MeOH}} \quad (26)$$

Thus, point selectivity values, S_{TAME} , were plotted against concentration of methanol as shown in Figure 10 to observe that the relation is very well valid. This suggests that the model is valid.

Conclusions

The synthesis of *tert*-amyl methyl ether by etherification of *tert*-amyl alcohol with methanol is addressed in this paper. Among the variety of catalysts used Amberlyst-36 was found

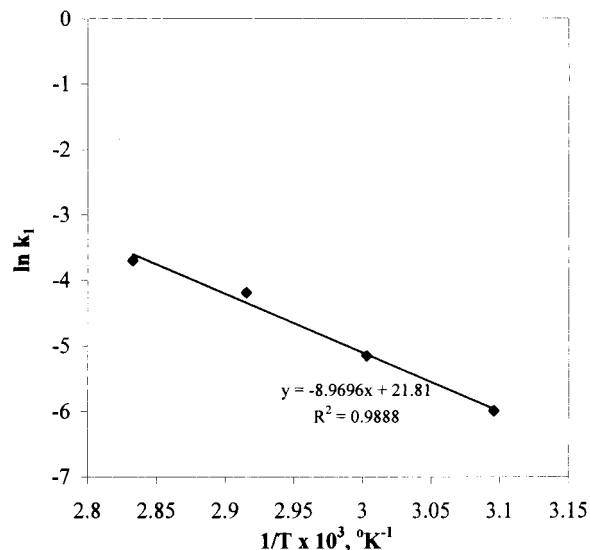


Figure 9. Arrhenius plot.

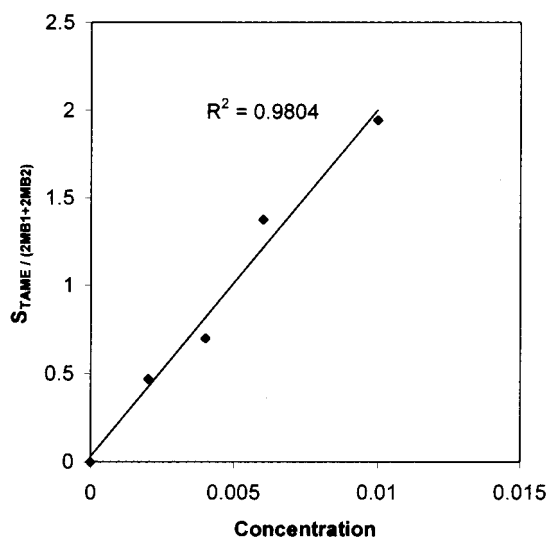


Figure 10. Selectivity of TAME as a Function of methanol concentration after 4 h.

to be the most efficient catalyst. The effects of various parameters on the rates of reaction were studied systematically to establish that there were no mass-transfer effects and that the overall reaction was found to be intrinsically kinetically controlled. The parallel reactions of *tert*-amyl alcohol adsorbed on the sites were found to control the overall rate of reaction which led to the formation of TAME, 2MB1, and 2MB2. The reaction follows pseudo first-order kinetics at a fixed catalyst loading. The selectivity of TAME over 2MB1 and 2MB2 is also found to be consistent with the model.

Acknowledgment

A.V.J. thanks AICTE for awarding Junior Research Fellowship. G.D.Y. thanks the Darbari Seth Professorship Endowment.

Note Added after ASAP: There were errors in the headings of Tables 3, 4, and 5 in the version posted ASAP June 8, 2001; the corrected version was posted July 20, 2001.

Received for review February 13, 2001.

OP010018+